



# Two novel SNPs rs1736952 and rs17354984 are highly associated with uveitis in ankylosing spondylitis

Ssu-Cheng Huang<sup>a</sup>, De-Kuang Hwang<sup>a,b</sup>, Wei-Chieh Fang<sup>c</sup>, Ai-Ru Hsieh<sup>d</sup>, Mei-Lin Shih<sup>e</sup>, Zi-Qing Zhuang<sup>e</sup>, Chong-En Gao<sup>e,f</sup>, Tai-Chi Lin<sup>a,b</sup>, Shih-Jen Chen<sup>a,b</sup>, Chih-Chien Hsu<sup>a,b,\*</sup>

<sup>a</sup>School of Medicine, National Yang Ming Chiao Tung University, Taipei, Taiwan, ROC; <sup>b</sup>Department of Ophthalmology, Taipei Veterans General Hospital, Taipei, Taiwan, ROC; <sup>c</sup>Department of Medical Education, Taipei Veterans General Hospital, Taipei, Taiwan, ROC; <sup>d</sup>Department of Statistics, Tamkang University, New Taipei City, Taiwan, ROC; <sup>e</sup>Department of Medical Research, Taipei Veterans General Hospital, Taipei, Taiwan, ROC; <sup>f</sup>Institute of Clinical Medicine, College of Medicine, National Yang Ming Chiao Tung University, Taipei, Taiwan, ROC

### Abstract

**Background:** Noninfectious anterior uveitis shares genetic factors, including HLA-B27, with ankylosing spondylitis (AS). The aim of this study was to identify significant single nucleotide polymorphisms (SNPs) associated with noninfectious anterior uveitis in AS patients, which may help predict the risk of developing this condition and provide deeper insights into its genetic basis.

**Methods:** A genome-wide association study (GWAS) was conducted using the genomic data of 468 AS patients, including 90 with noninfectious anterior uveitis and 378 without it, from the Taiwan Precision Medicine Initiative. This study identified relevant genes using SnpXplorer and developed a polygenic risk score (PRS) model to identify AS patients with an increased risk of noninfectious anterior uveitis. Biological pathways were analyzed via Enrichr-KG and various databases.

**Results:** GWAS revealed two novel SNPs, rs1736952 and rs17354984, with  $p$  values  $< 5 \times 10^{-8}$ , and 74 SNPs with  $p$  values  $< 1 \times 10^{-4}$ . The associated genes were involved mainly in antigen presentation, interferon signaling, immune regulation pathways, ciliary movement, and neurodegeneration. An optimal PRS model was constructed using 19 SNPs, achieving an area under the curve (AUC) of 0.907.

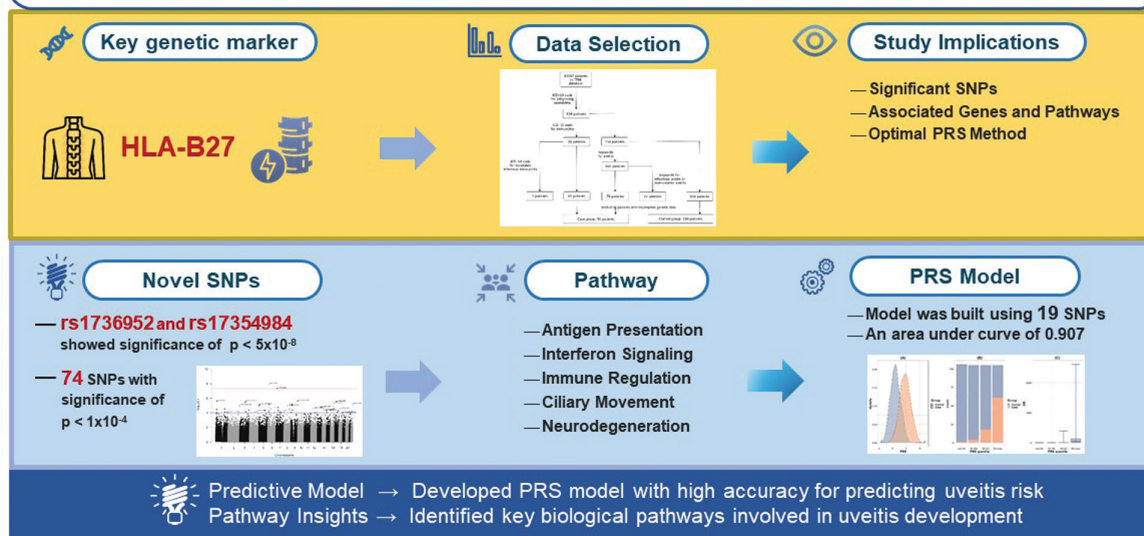
**Conclusion:** Our results revealed that two novel and significant SNP loci, rs1736952 and rs17354984, are strongly associated with noninfectious anterior uveitis in patients with AS. However, their roles in uveitis and other immune disorders warrant further investigation.

**Keywords:** Ankylosing spondylitis; Genome-wide association study; Genetic risk score; Uveitis

### Graphical abstract

#### Two Novel SNPs Rs1736952 and Rs17354984 Are Highly Associated with Uveitis in Ankylosing Spondylitis

##### Identify significant SNPs associated with non-infectious anterior uveitis in AS patients



Hsu CC et al. | Journal of the Chinese Medical Association (JCMA) 2025;88(3).

## 1. INTRODUCTION

Uveitis is an inflammation of the uvea, which includes the iris, ciliary body, and choroid. Uveitis can be classified based on anatomical location into anterior, intermediate, posterior, and panuveitis, and based on etiology into noninfectious and infectious types.<sup>1</sup> Uveitis accounts for approximately 5% to 10% of visual impairments worldwide.<sup>2</sup> If left untreated or inadequately managed, uveitis can lead to complications such as posterior synechiae, ocular hypertension, macular edema, cataracts, and glaucoma.<sup>3</sup>

Ankylosing spondylitis (AS) and uveitis are closely linked due to shared genetic immunological factors.<sup>4</sup> A significant proportion of AS patients develop uveitis, particularly noninfectious anterior uveitis, a common complication of the disease.<sup>5</sup> This strong association is largely attributed to the presence of the HLA-B27 antigen, which is prevalent in both AS and uveitis. The shared genetic factor of HLA-B27 suggests that both AS and noninfectious anterior uveitis may result from similar underlying genetic predispositions and immune system dysregulation. In fact, other genetic associations, such as ERAP-1, IL-23R, rs653778 of IFNA13, and rs28383797 of IFNA1, were discovered in previous studies.<sup>4,6,7</sup> Other studies have investigated cytokines and chemokines in HLA-B27+ AS-associated anterior uveitis patients to better understand this disease.<sup>8</sup>

Genome-wide association studies (GWASs) are powerful tools for identifying genetic variants associated with diseases by scanning the genomes of large cohorts.<sup>9</sup> This approach has been widely used in medical research to identify genetic risk factors for various conditions, including complex diseases such as diabetes, cancer, and autoimmune disorders.<sup>10-12</sup> These studies can highlight previously unknown genetic factors, offering new directions for biological pathways and potential therapeutic interventions.<sup>13</sup>

The aim of this study was to identify significant genetic factors associated with noninfectious anterior uveitis in AS patients. We conducted a GWAS using large amounts of genomic data from the Taiwan Precision Medicine Initiative (TPMI) (accessed on July 8, 2023), a large database consisting of genetic profiles and deidentified health information from one million volunteers from medical centers across Taiwan, and discovered significant and novel single nucleotide polymorphisms (SNPs) in AS patients with noninfectious anterior uveitis. An optimal polygenic risk score (PRS) model was developed, which revealed the genetic variants involved in noninfectious anterior uveitis comorbidity in AS patients and effectively predicted AS patients with increased risks of noninfectious anterior uveitis. The tools SnpXplorer and Enrichr-KG were used to explore the associated genes and biological pathways to explore the biological significance of the SNPs.<sup>14,15</sup> Our most significant finding is the identification of two novel and highly significant SNP loci, rs1736952 and rs17354984 ( $p < 5 \times 10^{-8}$ ), which are strongly associated with noninfectious anterior uveitis in AS patients. Genes associated with rs1736952 are linked to immune pathways such as antigen presentation and T-cell regulation, whereas genes related to rs17354984 are more closely connected to ciliary movement and neurodegeneration. The optimal PRS model effectively predicted a greater risk for noninfectious anterior uveitis in AS

patients, with an area under the curve (AUC) of 0.907 in the training set and 0.703 in the testing set.

## 2. METHODS

### 2.1. Study population

This study utilized genetic data from the TPMI (accessed on July 8, 2023), a database containing genetic profiles and de-identified health information from one million volunteers across medical centers in Taiwan.<sup>16</sup> The genotyping chip used in the TPMI database is a modified version of the Axiom Genome-Wide TWB (Taiwan Biobank) 2.0 Array Plate (Affymetrix, Santa Clara, CA).<sup>16</sup> Owing to the TPMI's data management policies, the data were limited to Taipei Veterans General Hospital participants. A total of 83 597 patients were recruited from Taipei Veterans General Hospital from 2014 to 2023 from the TPMI database. Data collection was approved by the Institutional Review Board of Taipei Veterans General Hospital, Taipei, Taiwan (TPEVGH IRB No: 2023-11-007ACF).

Patients with both AS and noninfectious anterior uveitis were selected as the case group, and patients with AS without uveitis composed the control group. Fig. 1 shows the flowchart for patient selection.

From a cohort of 83,597 individuals, we first identified 808 AS patients using the International Classification of Diseases (ICD)-10 code M45. Among these patients, 70 patients with anterior uveitis were selected using the ICD-10 code H20 for iridocyclitis. We then excluded five patients with secondary infectious iridocyclitis via the ICD-10 code H20.03, resulting in 65 patients in the case group. From the 738 AS patients without the ICD-10 code for iridocyclitis, we further searched the electronic medical records for keywords indicative of uveitis ("AAU," "uveitis," "iridocyclitis," "cyclitis," "Harada," "Fuch," "VKS," "Vogt-Kayanagi," "Vogt," "Kayanagi," "hypopyon," "glaucomacyclitic," "lens-induced," "endophthalmitis," "panophthalmitis," "panuveitis," "ophthalmia," "nodosa," "planitis," "vitreous abscess," "chorioretinitis," "retinitis," "choroiditis," "vasculitis," "uveitis due to secondary syphilis," "syphilitic uveitis," "retinochoroiditis," "acute retinal necrosis," "CMV retinitis," "PORN," "retinal necrosis," "ARN," "toxoplasmosis," "ocular tuberculosis," "ocular TB," "sarcoidosis," and "Behcet") and identified 100 additional patients. We then excluded 22 patients via keywords indicative of infectious uveitis or nonanterior uveitis ("Harada," "Fuch," "VKS," "Vogt-Kayanagi," "Vogt," "Kayanagi," "glaucomacyclitic," "lens-induced," "endophthalmitis," "panophthalmitis," "panuveitis," "ophthalmia," "nodosa," "planitis," "vitreous abscess," "chorioretinitis," "retinitis," "choroiditis," "vasculitis," "uveitis due to secondary syphilis," "syphilitic uveitis," "retinochoroiditis," "acute retinal necrosis," "CMV retinitis," "PORN," "retinal necrosis," "ARN," "toxoplasmosis," "ocular tuberculosis," "ocular TB," "sarcoidosis," and "Behcet"), resulting in an additional 78 patients for the case group. The final case group consisted of 143 patients. From the 738 AS patients without the ICD-10 code for iridocyclitis, the 638 patients whose electronic medical records did not contain keywords indicative of uveitis were selected as the control group.

A total of 781 patients were identified from the TPMI database, comprising 143 in the case group and 638 in the control group. Before quality control (QC), 700 522 SNPs were identified across the 781 patients.

### 2.2. Quality control

A total of 143 and 638 patients were initially selected for the case and control groups, respectively. After patients with incomplete genetic data were excluded, the final control and case groups comprised 91 and 380 patients, respectively, for a total

\*Author correspondence. Dr. Chih-Chien Hsu, Department of Ophthalmology, Taipei Veterans General Hospital, 201, Section 2, Shi-Pai Road, Taipei 112, Taiwan, ROC. E-mail address: chihchienym@gmail.com (C.-C.Hsu).

Conflicts of interest: The authors declare that they have no conflicts of interest related to the subject matter or materials discussed in this article.

Journal of Chinese Medical Association. (2025) 88: 211-221.

Received October 16, 2024; accepted December 8, 2024.

doi: 10.1097/JCMA.0000000000001210

Copyright © 2025, the Chinese Medical Association. This is an open access article under the CC BY-NC-ND license (<http://creativecommons.org/licenses/by-nc-nd/4.0/>)

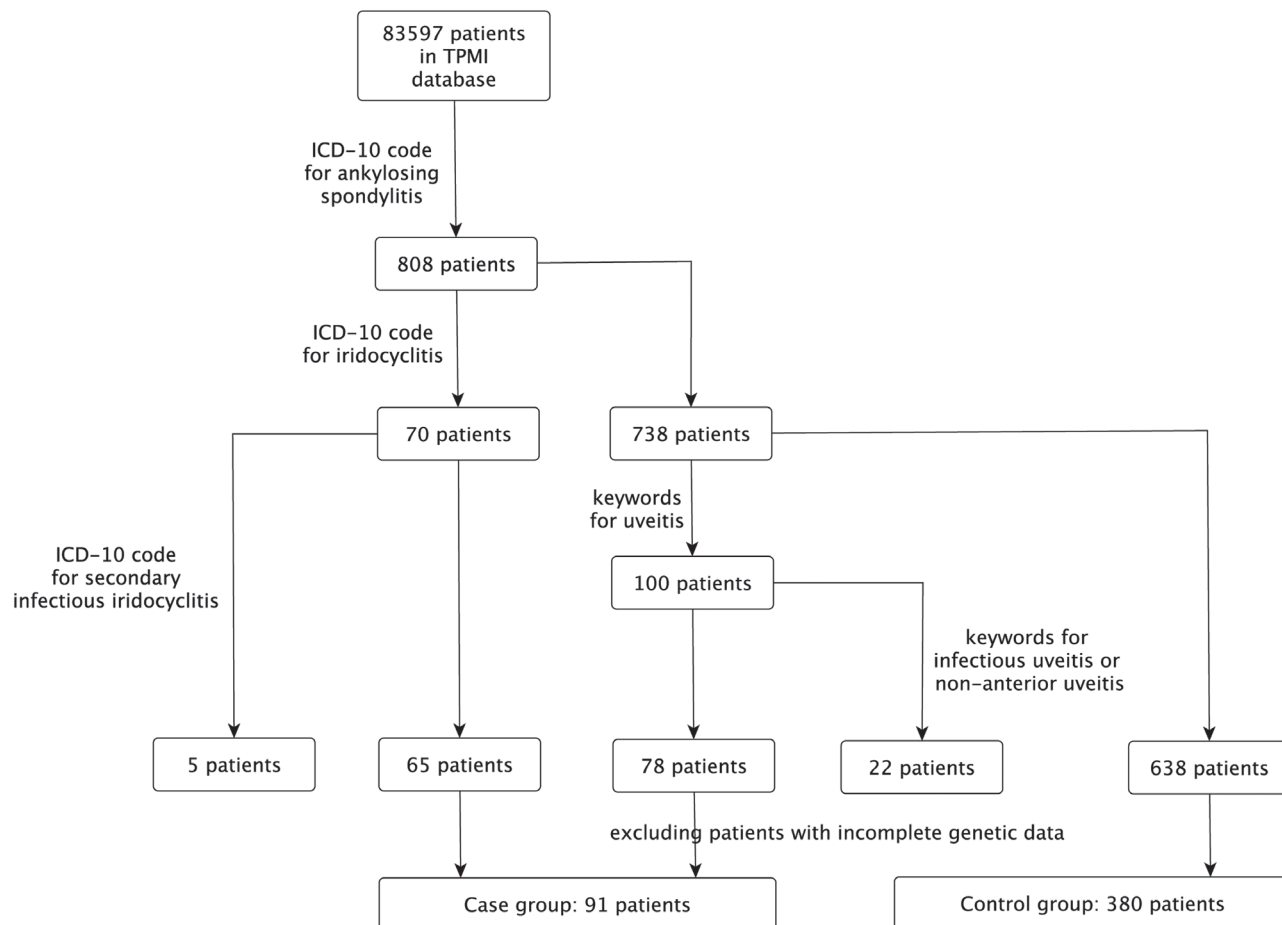


**Fig. 1** TPMI sample selection flowchart. Flowchart illustrating the criteria and number of patients selected in this study. The patients in the case group were ankylosing spondylitis patients with noninfectious anterior uveitis. The control group included ankylosing spondylitis patients without uveitis. ICD-10 = 10th revision of the International Classification of Diseases; TPMI = Taiwan Precision Medicine Initiative.

of 471 individuals. QC was conducted through eight steps via PLINK software (version 1.9) to exclude patients with high SNP missing rates (>5% missing data) and high heterozygosity rates (>3 standard deviations from the mean)<sup>17</sup> and to remove SNPs in linkage disequilibrium (LD), with >5% missing data, deviating from Hardy-Weinberg equilibrium ( $p$  value  $<1 \times 10^{-5}$ ), with different missing rates between groups, and with minor allele frequency (MAF)  $<0.01$  across all participants. After QC, the initial 471 patients were reduced to 468 (90 in the case group and 378 in the control group), and the number of SNPs was reduced from 700 522 to 268 240.

### 2.3. Genome-wide association study

A GWAS was conducted with PLINK v1.9 using QC-processed data to identify genetic factors in the case group compared with the control group. We applied the thresholds of a  $p$  value  $<5 \times 10^{-8}$  and a  $p$  value  $<1 \times 10^{-4}$  to identify significant SNPs in non-infectious anterior uveitis in the context of AS.

### 2.4. PRS model

To develop and evaluate PRSs, we randomly divided the processed genetic data from cases and controls into training and testing sets. Three different data partitioning ratios were applied: 9:1, 8:2, and 5:5. A GWAS was performed on the training set to obtain

summary statistics, which were then used in PRSice-2 software for PRS model training. The computations were performed using the C + T method, the default approach in PRSice-2, to develop the optimal PRS model. In addition, individual-level data such as age and sex were included as covariates in the computation. After the PRS model was built, a receiver operating characteristic (ROC) curve was generated, and the AUC was calculated. A density plot was used to visualize the results. Multiple random splits (20-30 times) were performed for each proportion (9:1, 8:2, 5:5) via the caret package in R, and the PRS model with the best AUC and density plot results was selected as the optimal PRS model.

### 2.5. Associated genes and biological pathway enrichment analysis

Both the significant SNPs from the GWAS and the SNPs used in the optimal PRS model were annotated via the online tool SnpXplorer to obtain information about their associated genes and previous research correlations, facilitating pathway analysis to explore their biological significance. Enrichment analysis was performed using Enrichr-KG to investigate associations between specific genes or gene sets and biological pathways. This analysis was based on databases including the Gene Ontology Biological Process (GOBP), Kyoto Encyclopedia of Genes and Genomes (KEGG, version 2021 Human), Reactome (version 2022), and the GWAS Catalog.<sup>18-20</sup> In addition, significant SNPs from the GWAS were cross-referenced with the literature and the UVEOGENE

database to determine if these SNPs had been previously identified, ensuring continuity with past research.<sup>21</sup> The datasets were accessed on July 8, 2023.

### 3. RESULTS

#### 3.1. Patient characteristics

A total of 468 patients, including 90 in the case group and 378 in the control group after QC, with a total of 268 240 SNPs, were included in the GWAS. The optimal PRS model was built with the data of 84 patients in the case group and 337 patients in the control group; among them, 65 (77%) and 208 (62%) were men, respectively, with a *p* value of 0.007. The mean ages of the two groups were  $52.33 \pm 13.93$  and  $51.25 \pm 15.10$  years, respectively, with a *p* value of 0.4.

#### 3.2. Noninfectious anterior uveitis risk loci in AS patients

A GWAS was conducted to identify significant genetic factors associated with noninfectious anterior uveitis in AS patients. The GWAS results are visualized in a Manhattan plot (Fig. 2).

Two SNPs, rs1736952 (MAF = 0.051 in the case group, odds ratio [OR] = 39.89) on chromosome 6 and rs17354984 (MAF = 0.084 in the case group, OR = 7.597) on chromosome 7, showed genome-wide significance, with a *p* value  $< 5 \times 10^{-8}$  (Table 1). A total of 74 SNPs had *p* values  $< 1 \times 10^{-4}$  (Table 2). These SNPs are considered noninfectious anterior uveitis risk loci in AS patients.

#### 3.3. PRS and the optimal PRS model

To predict AS patients with higher risks of noninfectious anterior uveitis, we built the optimal PRS model by using a 9:1 training-to-testing ratio trained with 84 and 337 patients in the case and control groups, respectively. This model incorporated 19 SNPs (Table 3) from the 74 significant (*p* value  $< 5 \times 10^{-4}$ ) SNPs.

The mean PRS in AS patients with noninfectious anterior uveitis was significantly greater than that in noninfectious anterior uveitis patients, with a *p* = 0.0125 (Fig. 3A), indicating the association of the 19 SNPs with noninfectious anterior uveitis comorbidity in AS patients. The risk of uveitis increases with higher PRS values (Fig. 3B, C). Patients in the Q3-maximum, Q2-3, and Q1-2 PRS quantiles had a 145.57-, 21.72-, and

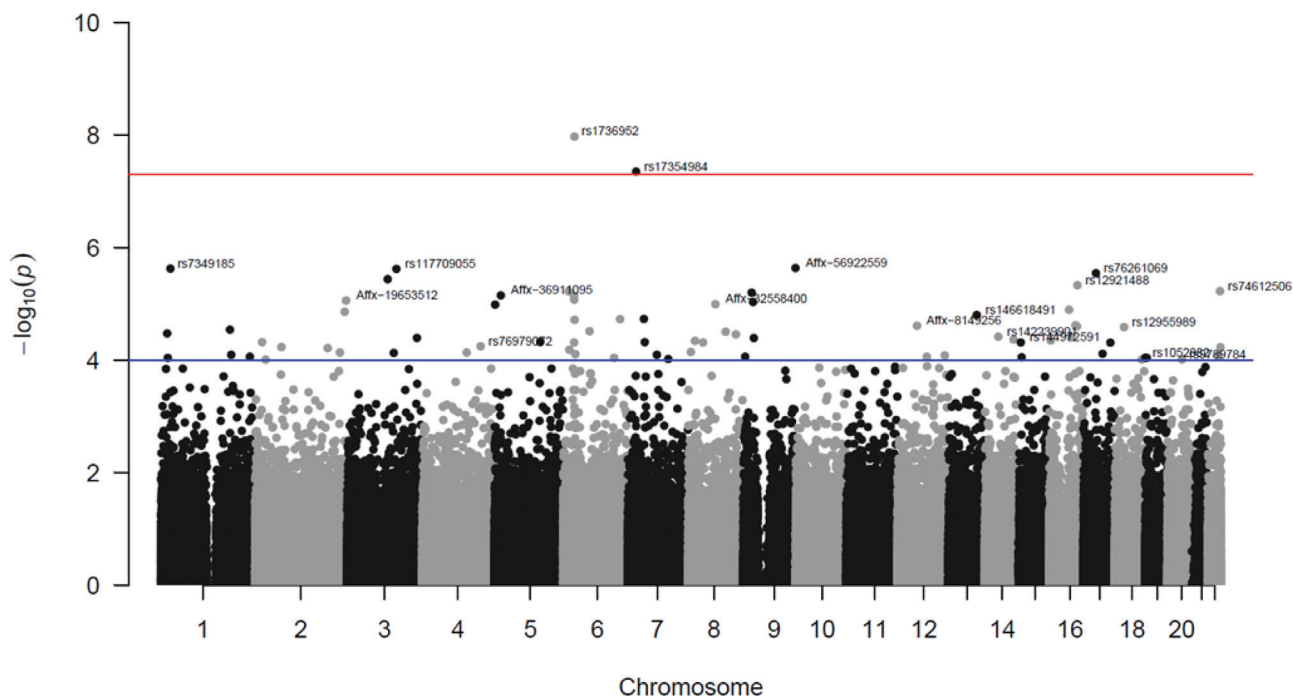


**Fig. 2** Manhattan plot of the GWAS. The Manhattan plot (90 cases, 378 controls) illustrates SNPs associated with uveitis in AS patients. The red line represents the genome-wide significance threshold of a *p* value  $< 5 \times 10^{-8}$ , and the blue line represents the threshold of a *p* value  $< 1 \times 10^{-4}$ . Two SNPs, rs1736952 on chromosome 6 and rs17354984 on chromosome 7, reached the genome-wide significance threshold of a *p* value  $< 5 \times 10^{-8}$ . A total of 74 SNPs reached the genome-wide significance threshold of a *p* value  $< 1 \times 10^{-4}$ . AS = ankylosing spondylitis; GWAS = genome-wide association study; SNP = single nucleotide polymorphism.

**Table 1**  
Two SNPs with *p* values  $< 5 \times 10^{-8}$

SNP	CHR	Position	MAF (in cases)	MAF (in controls)	<i>p</i>	OR	Gene symbol
rs1736952	6	29817876	0.05056	0.001333	$1.07 \times 10^{-8}$	39.89	<i>NRM, HCG4, HLA-V, ABCF1, TRIM31, RNF39, PPP1R11, HLA-J, ZNRD1ASP, HCG9, HLA-G, HLA-F, ZFP57, TRIM27, HLA-H, HLA-A, HLA-F-AS1, MCCD1P2, HCG4B, HCG20, HLA-U, MICD, HLA-K, PAIP1P1, ZDHC20P1, IFITM4P, DDX39BP2, RPL23AP1, HLA-P, HCG17, MICE, HCP5B</i>
rs17354984	7	21742645	0.08427	0.01197	$4.48 \times 10^{-8}$	7.597	<i>DNAH11</i>

CHR = chromosome; MAF = minor allele frequency; OR= odds ratio; SNP = single nucleotide polymorphisms.

**Table 2****Seventy-four significant SNPs with  $p$  values  $<1 \times 10^{-4}$** 

SNP	CHR	Position	MAF (in cases)	MAF (in controls)	$p$	OR	Gene symbol
rs1736952	6	29817876	0.05056	0.001333	$1.07 \times 10^{-8}$	39.89	<i>HLA-G, MICF</i>
rs17354984	7	21742645	0.08427	0.01197	$4.48 \times 10^{-8}$	7.597	<i>DNAH11</i>
Affx-56922559	9	137712385	0.05618	0.006631	$2.30 \times 10^{-6}$	8.917	<i>COL5A1</i>
rs7349185	1	25805163	0.1236	0.03581	$2.36 \times 10^{-6}$	3.797	<i>TMEM57</i>
rs117709055	3	130088948	0.05618	0.006649	$2.39 \times 10^{-6}$	8.893	<i>COL6A5</i>
rs76261069	17	33207596	0.1124	0.0305	$2.84 \times 10^{-6}$	4.023	<i>CCT6B</i>
Affx-20867811	3	107058830	0.05056	0.005305	$3.64 \times 10^{-6}$	9.985	<i>CCDC54</i>
rs12921488	16	74291233	0.0618	0.009284	$4.67 \times 10^{-6}$	7.029	<i>PSMD7</i>
rs74612506	22	47938038	0.04651	0.004155	$5.94 \times 10^{-6}$	11.69	<i>TBC1D22A</i>
rs79284941	6	14628325	0.1461	0.05053	$5.96 \times 10^{-6}$	3.214	<i>CD83</i>
rs864347	9	22185093	0.08989	0.02128	$6.31 \times 10^{-6}$	4.543	<i>CDKN2A, CDKN2B</i>
Affx-36911095	5	17242812	0.1236	0.03846	$7.06 \times 10^{-6}$	3.526	<i>BASP1</i>
rs2531818	6	28485325	0.05682	0.007958	$7.17 \times 10^{-6}$	7.51	<i>GPX6</i>
rs9257792	6	29366662	0.05618	0.007958	$8.39 \times 10^{-6}$	7.421	<i>OR12D3, OR12D2, OR5V1</i>
Affx-19653512	2	239614985	0.05618	0.007979	$8.70 \times 10^{-6}$	7.401	<i>LOC100287387</i>
Affx-33583936	9	25863318	0.1124	0.03316	$9.26 \times 10^{-6}$	3.691	<i>TUSC1, LOC100506422</i>
Affx-32558400	8	71731027	0.09091	0.02255	$1.01 \times 10^{-5}$	4.335	<i>XKR9</i>
Affx-26319870	5	2301371	0.09659	0.02527	$1.03 \times 10^{-5}$	4.125	<i>IRX4</i>
rs72805440	16	52379574	0.0625	0.01067	$1.27 \times 10^{-5}$	6.183	<i>TOX3</i>
Affx-70125822	2	235924552	0.0618	0.01061	$1.38 \times 10^{-5}$	6.142	<i>SH3BP4</i>
rs146618491	13	93772274	0.05056	0.006667	$1.57 \times 10^{-5}$	7.935	<i>GPC6</i>
rs150434741	7	42232504	0.09659	0.02653	$1.85 \times 10^{-5}$	3.924	<i>GLI3</i>
rs117016917	6	150111225	0.06742	0.01326	$1.87 \times 10^{-5}$	5.378	<i>PCMT1</i>
rs73425422	6	30262369	0.04762	0.00551	$1.92 \times 10^{-5}$	9.025	<i>TRIM39, TRIM39-RPP21, RPP21, HCG18</i>
rs117886821	16	69358909	0.07865	0.01857	$2.40 \times 10^{-5}$	4.512	<i>SNTB2, VPS4A, PDF, COG8, NIP7, TMED6</i>
Affx-8149256	12	51489354	0.04494	0.005305	$2.45 \times 10^{-5}$	8.824	<i>TFCP2</i>
rs75428604	16	73269528	0.07865	0.01862	$2.50 \times 10^{-5}$	4.5	<i>C16orf47</i>
rs12955989	18	24106190	0.07865	0.2162	$2.58 \times 10^{-5}$	0.3095	<i>KCTD1</i>
rs186845124	1	182327274	0.04494	0.005376	$2.87 \times 10^{-5}$	8.706	<i>GLUL</i>
rs28600278	6	69628538	0.04167	0.004132	$3.06 \times 10^{-5}$	10.48	<i>ADGRB3, BAI3</i>
rs77847061	8	98823474	0.1854	0.0809	$3.13 \times 10^{-5}$	2.586	<i>LAPTM4B</i>
rs12096215	1	17224893	0.5674	0.3963	$3.35 \times 10^{-5}$	1.998	<i>CROCC, RNU1-2</i>
rs62521632	8	125709909	0.1307	0.04667	$3.48 \times 10^{-5}$	3.071	<i>MTSS1</i>
rs142239901	14	54594533	0.03933	0.003979	$3.84 \times 10^{-5}$	10.25	<i>BMP4</i>
rs189232287	16	57911973	0.03933	0.003989	$3.95 \times 10^{-5}$	10.22	<i>KIFC3, CNGB1</i>
rs117292774	3	184145500	0.1404	0.05319	$4.03 \times 10^{-5}$	2.908	<i>CLCN2, POLR2H, THPO, CHR1, EIF2B5</i>
rs10968154	9	27862445	0.09551	0.02785	$4.04 \times 10^{-5}$	3.686	<i>LINGO2</i>
rs11844301	14	94766718	0.1798	0.07846	$4.29 \times 10^{-5}$	2.574	<i>SERPINA6</i>
rs11076811	16	4128510	0.1573	0.064	$4.48 \times 10^{-5}$	2.73	<i>ADCY9</i>
rs144407323	8	17870922	0.06742	0.01463	$4.55 \times 10^{-5}$	4.87	<i>PCM1</i>
rs147495637	5	121366814	0.08427	0.02255	$4.75 \times 10^{-5}$	3.99	<i>SRFBP1</i>
rs4832420	2	18173220	0.07303	0.01724	$4.79 \times 10^{-5}$	4.491	<i>KCNS3</i>
Affx-30491770	7	44572855	0.07303	0.01724	$4.79 \times 10^{-5}$	4.491	<i>NPC1L1</i>
rs6933672	6	28973911	0.05056	0.007958	$4.85 \times 10^{-5}$	6.639	<i>ZNF311</i>
rs185853321	8	38917423	0.05056	0.007958	$4.85 \times 10^{-5}$	6.639	<i>ADAM9</i>
rs144972591	15	26864741	0.05056	0.007958	$4.85 \times 10^{-5}$	6.639	<i>GABRB3</i>
rs12947919	17	71121946	0.07865	0.01989	$4.89 \times 10^{-5}$	4.206	<i>SLC39A11, SSTR2, COG1</i>
rs76979072	4	153960451	0.05056	0.008065	$5.67 \times 10^{-5}$	6.55	<i>FHDC1</i>
rs76824549	2	69162005	0.118	0.04111	$5.85 \times 10^{-5}$	3.12	<i>GKN2</i>
rs140214134	22	49123512	0.05747	0.0107	$5.90 \times 10^{-5}$	5.64	<i>FAM19A5</i>
rs73982684	2	191165894	0.118	0.04122	$6.13 \times 10^{-5}$	3.111	<i>HIBCH</i>
rs9396669	6	16399176	0.4944	0.3342	$6.53 \times 10^{-5}$	1.948	<i>ATXN1</i>
rs2741673	8	6941449	0.1404	0.2851	$7.16 \times 10^{-5}$	0.4096	<i>DEFA3, DEFA5</i>
rs74441014	4	117311047	0.05618	0.01064	$7.31 \times 10^{-5}$	5.536	<i>TRAM1L1</i>
rs139664253	2	223276572	0.09551	0.02926	$7.33 \times 10^{-5}$	3.504	<i>SGPP2</i>
rs75461080	3	123164453	0.08523	0.02387	$7.44 \times 10^{-5}$	3.81	<i>ADCY5</i>
rs9890089	17	50608431	0.1105	0.03714	$7.70 \times 10^{-5}$	3.22	<i>CA10</i>
rs3096696	6	32154695	0.04545	0.006631	$7.81 \times 10^{-5}$	7.133	<i>AGER</i>
rs148512981	1	185738115	0.07955	0.02122	$8.04 \times 10^{-5}$	3.986	<i>HMCN1</i>
rs78007164	7	76369091	0.07955	0.02122	$8.04 \times 10^{-5}$	3.986	<i>SPDYE18</i>
Affx-7054967	12	124301542	0.4101	0.2613	$8.24 \times 10^{-5}$	1.966	<i>DNAH10</i>

(Continued)

**Table 2**  
Continued

SNP	CHR	Position	MAF (in cases)	MAF (in controls)	p	OR	Gene symbol
rs5764547	22	44123071	0.2022	0.09682	$8.25 \times 10^{-5}$	2.365	<i>EFCAB6</i>
rs61837322	1	234961493	0.0618	0.01326	$8.69 \times 10^{-5}$	4.901	<i>IRF2BP2</i>
rs74308888	9	5165324	0.0618	0.01326	$8.69 \times 10^{-5}$	4.901	<i>INSL6</i>
rs149037470	12	76984009	0.0618	0.01326	$8.69 \times 10^{-5}$	4.901	<i>OSBPL8</i>
rs77749096	15	29191308	0.04494	0.006631	$8.85 \times 10^{-5}$	7.049	<i>APBA2</i>
rs1052882	19	463528	0.3876	0.2427	$9.01 \times 10^{-5}$	1.975	<i>SHC2, ODF3L2, C2CD4C</i>
rs28488609	1	18852250	0.125	0.04642	$9.10 \times 10^{-5}$	2.935	<i>KLHDC7A</i>
rs56051417	6	134243665	0.04494	0.006649	$9.10000 \times 10^{-5}$	7.031	<i>TCF21, TBPL1, SLC2A12</i>
rs189769231	19	3779682	0.1071	0.03523	$9.10 \times 10^{-5}$	3.286	<i>APBA3, MRPL54, RAX2, MATK, ZFR2</i>
rs73200084	7	106502325	0.06742	0.01592	$9.55 \times 10^{-5}$	4.47	<i>PIK3CG</i>
rs148456362	18	70727519	0.07303	0.01857	$9.74 \times 10^{-5}$	4.165	<i>NETO1, LOC100505797</i>
rs9789784	20	38200784	0.07303	0.01857	$9.74 \times 10^{-5}$	4.165	<i>MAF1</i>
rs8179206	2	27497575	0.07865	0.02128	$9.79 \times 10^{-5}$	3.927	<i>DNAJC5G</i>

CHR = chromosome; SNP = single nucleotide polymorphism; MAF = minor allele frequency; OR = odds ratio.

**Table 3**

## Nineteen SNPs included in the optimal PRS model

SNP	CHR	Position	MAF (in cases)	MAF (in controls)	p	OR	Gene symbol
rs117064987	4	175000000	0.1566	0.06399	$1.01 \times 10^{-4}$	2.717	<i>FBXO8, CEP44</i>
rs117292774	3	184000000	0.1386	0.05373	$1.33 \times 10^{-4}$	2.833	<i>CLCN2, POLR2H, THPO, CHRD, EIF2B5</i>
rs5764547	22	44123071	0.1988	0.09375	$1.42 \times 10^{-4}$	2.398	<i>EFCAB6</i>
rs11076811	16	4128510	0.1566	0.06587	$1.61 \times 10^{-4}$	2.634	<i>ADCY9</i>
rs6486730	12	129000000	0.3313	0.494	$1.66 \times 10^{-4}$	0.5074	<i>TMEM132C</i>
rs11844301	14	94766718	0.1807	0.08209	$1.67 \times 10^{-4}$	2.467	<i>SERPINA6</i>
rs606316	11	129000000	0.4217	0.2738	$2.05 \times 10^{-4}$	1.934	<i>KCNJ1</i>
rs117406145	13	22299871	0.01807	0.1101	$2.37 \times 10^{-4}$	0.1487	<i>FGF9</i>
rs1052882	19	463528	0.3855	0.244	$2.44 \times 10^{-4}$	1.944	<i>SHC2, ODF3L2, C2CD4C</i>
Affx-31931112	8	23136285	0.1928	0.09254	$2.53 \times 10^{-4}$	2.342	<i>R3HCC1</i>
Affx-30915614	7	78209789	0.2711	0.1507	$2.56 \times 10^{-4}$	2.095	<i>MAGI2</i>
rs12625308	20	40695781	0.2108	0.1057	$2.61 \times 10^{-4}$	2.262	<i>PTPRT</i>
rs2289145	19	54193391	0.2229	0.1146	$2.67 \times 10^{-4}$	2.216	<i>DPRX, MIR519C</i>
Affx-21957861	3	195000000	0.4096	0.2657	$2.69 \times 10^{-4}$	1.918	<i>FAM43A</i>
rs16994839	20	14727707	0.2711	0.4254	$2.72 \times 10^{-4}$	0.5024	<i>MACROD2</i>
rs12977455	19	31465583	0.1566	0.06886	$3.14 \times 10^{-4}$	2.511	<i>LOC101927254</i>
rs12032930	1	190000000	0.3554	0.509	$3.93 \times 10^{-4}$	0.532	<i>BRINP3</i>
rs3744763	17	37730894	0.5904	0.4375	$4.08 \times 10^{-4}$	1.853	<i>CDK12</i>
Affx-12352968	16	1076543	0.3675	0.2336	$4.32 \times 10^{-4}$	1.906	<i>LMF1, SOX8, SSTR5, C1QTNF8</i>

CHR = chromosome; MAF = minor allele frequency; OR = odds ratio; PRS = polygenic risk score; SNP = single nucleotide polymorphism.

4.16-fold increased risk of anterior uveitis, respectively, compared with those in the minimum-Q1 quantile. The ROC curves illustrate the predictive performance of the optimal PRS model in the training and testing sets, yielding AUCs of 0.907 and 0.703, respectively (Fig. 4). The covariates (age and sex) yielded a predictive accuracy of AUC = 0.612 in the training set, which was significantly lower than that of the PRS model. Our optimal PRS model effectively distinguished AS patients at high risk of noninfectious anterior uveitis.

### 3.4. Associated genes and biological pathway enrichment analysis

Biological pathway enrichment analysis was conducted to identify pathways and diseases associated with SNP-related genes (Figs. 5 and 6). Annotation using SnpXplorer revealed that rs1736952 is an intergenic locus, not within any specific gene, but associated with the following genes: *NRM, HCG4, HLA-V, ABCF1, TRIM31, RNF39, PPP1R11, HLA-J, ZNRD1ASP, HCG9, HLA-G, HLA-F, ZFP57, TRIM27, HLA-H, HLA-A, HLA-F-AS1, MCCD1P2, HCG4B, HCG20, HLA-U, MICD,*

*HLA-K, PAIP1P1, ZDHHC20P1, IFITM4P, DDX39BP2, RPL23AP1, HLA-P, HCG17, MICE, and HCP5B.* Rs17354984 is located within the *DNAH11* gene. Enrichment analysis of the genes associated with the significant SNPs via Enrichr-KG identified relevant biological pathways in the GOBP, KEGG, and Reactome databases.

Genes associated with the key SNP rs1736952, particularly HLA-A, HLA-F, HLA-G, and TRIM31, are involved in major histocompatibility complex (MHC)-mediated antigen presentation, interferon signaling, and natural killer (NK) cell and T-cell immune regulation pathways. The related diseases are primarily infectious diseases, autoimmune diseases, and rejection responses, indicating that rs1736952-associated genes may play a role in the immune mechanisms of noninfectious anterior uveitis in AS. The gene *DNAH11*, in which rs17354984 is located, is more closely related to neurodegeneration and ciliary movement. Collectively, our results indicate that novel and significant SNP loci, rs1736952 and rs17354984, are strongly associated with noninfectious anterior uveitis comorbidity in patients with AS. Further investigation is needed to elucidate the

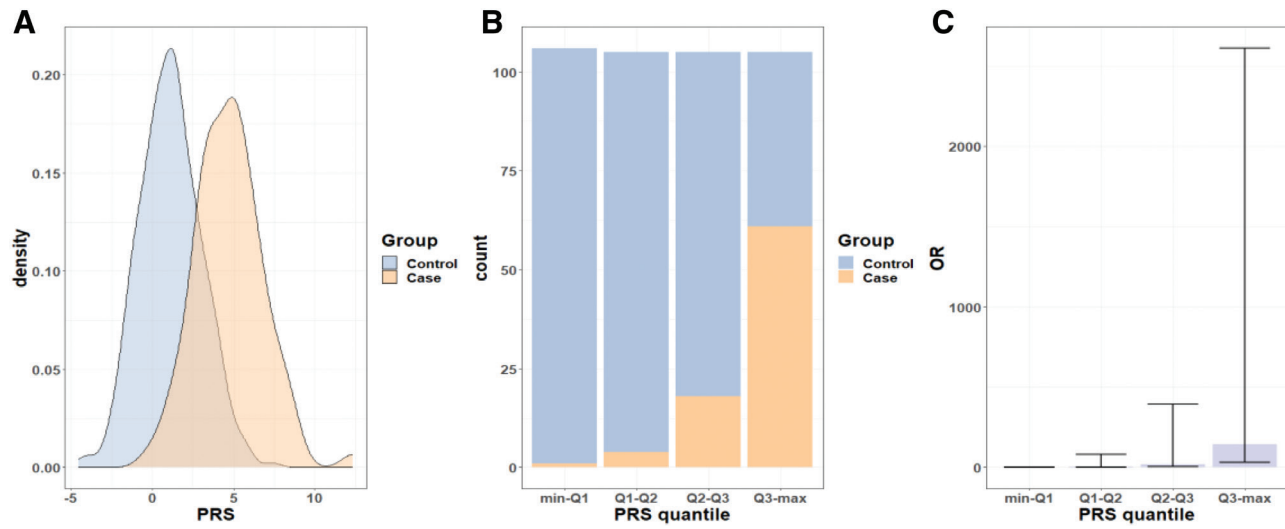


**Fig. 3** Risk of noninfectious anterior uveitis in the case and control groups, as shown by the PRS. A, The density plot shows the distribution of PRS scores for the case and control groups via the optimal PRS model. B, Distribution according to PRS quantiles. C, ORs for anterior uveitis according to PRS quantiles. OR = odds ratios; PRS = polygenic risk score.

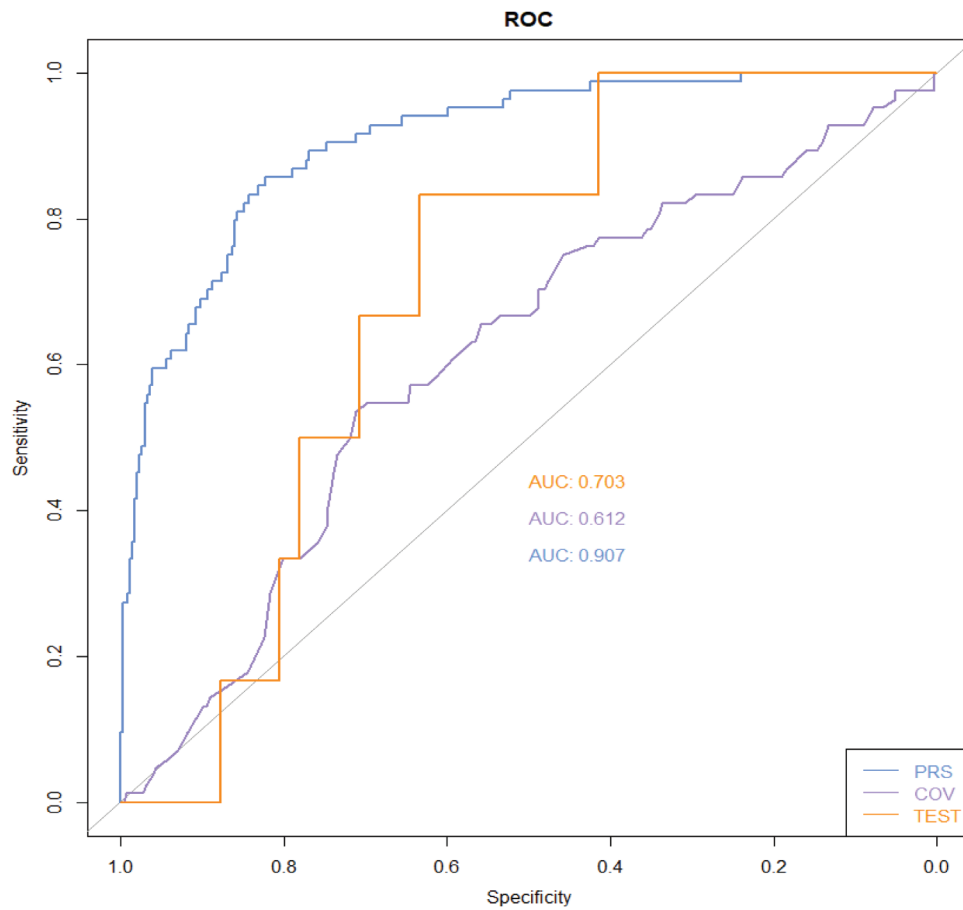


**Fig. 4** ROC curve for the optimal PRS model. The blue ROC curve shows the predictive accuracy of the optimal PRS model, with an AUC of 0.907 in the training set, whereas the orange line represents the predictive accuracy of the model in the testing set, with an AUC of 0.703. The purple line represents the predictive accuracy of covariates (sex, age), with an AUC of 0.612 in the training set. AUC = area under the curve; PRS = polygenic risk score; ROC = receiver operating characteristic.



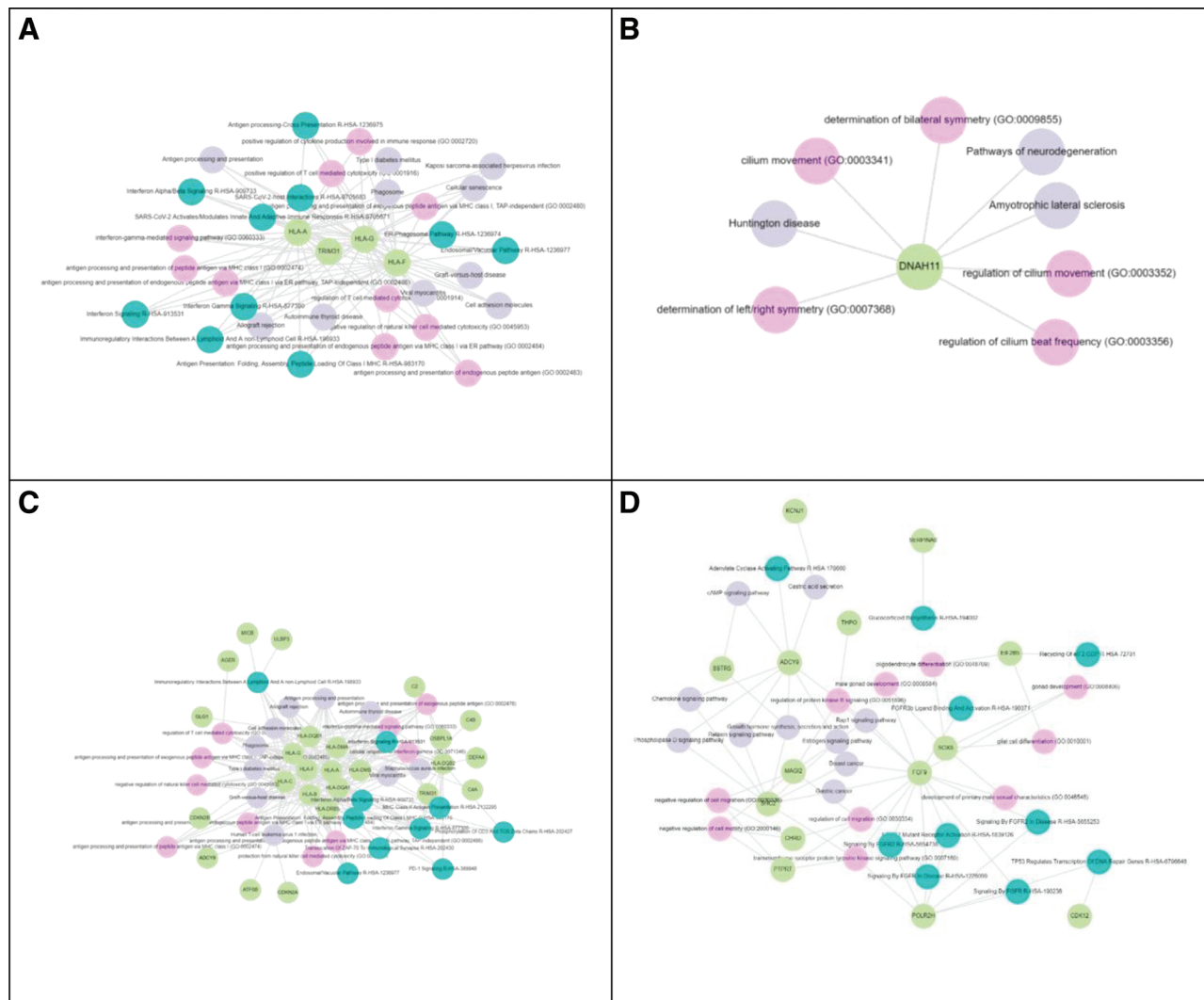


**Fig. 6** Network diagram of biological pathways related to the genes associated with the significant SNPs. Significant SNPs: (A) rs1736952, (B) rs17354984, (C) 74 significant SNPs with  $p$  values  $< 1 \times 10^{-4}$ , (D) 19 SNPs involved in the optimal PRS model. The light green circles represent the genes associated with the significant SNPs. The colors represent pathways in different databases: pink for GOBP, gray for KEGG, and teal for Reactome. GOBP = Gene Ontology Biological Process; KEGG = Kyoto Encyclopedia of Genes and Genomes; PRS = polygenic risk score; SNP = single nucleotide polymorphisms.

involved in antigen presentation, interferon signaling, and immune regulation, such as HLA-A, HLA-F, HLA-G, and TRIM31. According to GeneCards (accessed on July 8, 2023),<sup>22</sup> HLA-A, HLA-F, and HLA-G are MHC class I molecules involved in antigen presentation and CD8+ T-cell regulation. MHC class I risk alleles are associated with autoimmune diseases such as AS, psoriasis, and Behçet's disease.<sup>23</sup> In the human eye, Goverdhan et al<sup>24</sup> reported that HLA class I antigens were mostly observed in large vessels of the choroid. This suggests that HLA class I gene variants may be associated with autoimmune diseases of the choroid and could potentially affect other parts of the uvea. For example, approximately 50% of AS patients with acute anterior uveitis are HLA-B27 positive.<sup>25</sup> In addition, the HLA-A29 serotype was found to increase the risk of Birdshot uveitis, and it was hypothesized to be expressed in choroidal melanocytes, which are possible targets of autoreactive T cells.<sup>26</sup> TRIM31 is an E3 ubiquitin-protein ligase involved in antiviral responses and inflammation regulation. Abnormal TRIM31 expression can contribute to innate immune diseases by enhancing NLRP3 inflammasome activation.<sup>27,28</sup> Given the known immune dysregulation in noninfectious anterior uveitis

and AS, the variation at rs1736952 may play a specific role in the immune pathways of uveitis in AS.

The SNP rs17354984 exhibited an OR of 7.597. It is located in the *DNAH11* gene, which is associated with ciliary movement and neurodegeneration. Previous studies have identified associations between *DNAH11* and diseases such as ciliary dyskinesia, asthenozoospermia, congenital heart disease, and heterotaxy.<sup>29-31</sup> Some studies have reported associations between *DNAH11* and ovarian, breast, and esophageal squamous cell carcinoma.<sup>32,33</sup> Although the pathophysiology of *DNAH11* remains poorly understood, its role in uveitis is difficult to determine. In contrast to rs1736952, the biological pathways and functions of rs17354984 are not directly linked to uveitis. However, further analysis of genes and biological pathways associated with the 19 SNPs in the optimal PRS model revealed links to breast and gastric cancer. This finding suggests that genes associated with rs17354984 and the 19 SNPs in the PRS model may be involved in a shared biological mechanism, potentially related to immune pathways in both cancers.

The 19 SNPs in the optimal PRS model did not include the key findings, rs1736952 and rs17354984. This omission may be

due to the low frequencies (0.051 and 0.084 in the case group) of these two SNPs. However, their high odds ratios (ORs) (39.89 and 7.597) indicate that, despite their rarity, AS patients carrying these SNPs have a significantly increased risk of developing uveitis.

Our study had several limitations. This study had a relatively small sample size ( $n = 468$ ) and was limited to a single ethnic group, reducing its statistical power and highlighting the need for further validation of the PRS model in larger, multiethnic cohorts. The lack of an independent validation cohort and the use of TPMI samples for both training and testing may have led to overfitting and reduced generalizability. In addition, the cross-sectional design introduced potential errors, as control patients without noninfectious anterior uveitis might develop this condition in the future. Selection bias was also a concern, as the higher proportion of male participants, despite the greater prevalence of noninfectious uveitis in women, may have affected the representativeness of the findings.

Further studies with larger, more diverse cohorts are necessary to validate these findings and assess their broader applicability across different populations. Functional genomics and longitudinal studies are essential to establish causal relationships between these SNPs and noninfectious anterior uveitis in AS patients. Gene editing in cellular or animal models may provide insights into the roles of rs1736952 and other identified SNPs in disease pathogenesis.

Additionally, it is important to acknowledge the limitations of GWAS.<sup>34</sup> These studies often fail to identify specific causal variants and genes and may overlook relevant genetic factors influencing complex traits. The clinical predictive value of SNPs is limited, and GWASs based on SNP arrays are unable to detect extremely rare mutations that could contribute to the disease.

In conclusion, we performed a GWAS of AS patients with and without noninfectious anterior uveitis using genetic data from the TPMI database and identified two novel and significant SNP loci, rs1736952 and rs17354984, that are highly associated with noninfectious anterior uveitis comorbidity in AS patients. The rs1736952-related genes were associated with immune pathways such as antigen presentation and T-cell regulation, whereas the rs17354984-related genes were more related to ciliary movement and neurodegeneration. The roles of these two SNPs in uveitis, ocular diseases, AS, and other immune-related disorders require further investigation.

## ACKNOWLEDGMENTS

This study was supported by the Taipei Veterans General Hospital (V113C-201) and the Big Data Center, Taipei Veterans General Hospital (BDC, TPEVGH), Taiwan.

## REFERENCES

- Burkholder BM, Jabs DA. Uveitis for the non-ophthalmologist. *BMJ* 2021;372:m4979.
- Miserocchi E, Fogliato G, Modorati G, Bandello F. Review on the worldwide epidemiology of uveitis. *Eur J Ophthalmol* 2013;23:705–17.
- García-Aparicio A, Martín LA, Zamorano RQ, Lancho RL, Pérez LDO, Fernández SS, et al. Complications of uveitis in a Spanish population, UveCAM study. *Arch Soc Esp Ophthalmol* 2022;97:244–50.
- Liu JJ, Li HB, Lan T, Wang WN. IFNA1 and IFNA13 genes confer genetic predisposition to ankylosing spondylitis-associated uveitis in a Chinese population. *Curr Eye Res* 2021;46:585–91.
- Gouveia EB, Elmann D, Morales MS. Ankylosing spondylitis and uveitis: overview. *Rev Bras Reumatol* 2012;52:742–56.
- Wakefield D, Yates W, Amjadi S, McCluskey P. HLA-B27 Anterior uveitis: immunology and immunopathology. *Ocul Immunol Inflamm* 2016;24:450–9.
- Robinson PC, Leo PJ, Pointon JJ, Harris J, Cremin K, Bradbury LA, et al; Wellcome Trust Case Control Consortium. The genetic associations of acute anterior uveitis and their overlap with the genetics of ankylosing spondylitis. *Genes Immun* 2016;17:46–51.
- Li H, He ZX, Deng BL, Yang C, Wang L, Xiao J, et al. Cytokines and chemokines involved in HLA-B27-positive ankylosing spondylitis-associated acute anterior uveitis. *Mol Vis* 2023;29:378–85.
- Dehghan A. Genome-wide association studies. *Methods Mol Biol* 2018;1793:37–49.
- Shiota M, Tatarano S, Kamoto T, Matsuyama H, Sakai H, Igawa T, et al. Genome-wide association studies in advanced prostate cancer: KYUCOG-1401-a study. *Endocr Relat Cancer* 2023;30:e230044.
- Shojima N, Yamauchi T. Progress in genetics of type 2 diabetes and diabetic complications. *J Diabetes Investig* 2023;14:503–15.
- Kwon YC, Chun SW, Kim KW, Mak AS. Update on the genetics of systemic lupus erythematosus: genome-wide association studies and beyond. *Cells* 2019;8:1180.
- Visscher PM, Wray NR, Zhang Q, Sklar P, McCarthy MI, Brown MA, et al. 10 years of GWAS discovery: biology, function, and translation. *Am J Hum Genet* 2017;101:5–22.
- Tesi N, Lee SVD, Hulsman M, Holstege H, Reinders MJ. SnpXplorer: a web application to explore human SNP-associations and annotate SNP-sets. *Nucleic Acids Res* 2021;49:w603–12.
- Evangelista JE, Xie ZR, Marino GB, Nguyen N, Clarke DJB, Ma'ayan A. Enrichr-KG: bridging enrichment analysis across multiple libraries. *Nucleic Acids Res* 2023;51:W168–79.
- Taiwan Precision Medicine Initiative. <https://tpmi.ibms.sinica.edu.tw/www/>. Accessed July 8, 2023.
- Purcell P, Neale B, Todd-Brown K, Thomas L, Ferreira MAR, Bender D, et al. PLINK: a tool set for whole-genome association and population-based linkage analyses. *Am J Hum Genet* 2007;81:559–75.
- Kanehisa M, Goto S. KEGG: Kyoto encyclopedia of genes and genomes. *Nucleic Acids Res* 2000;28:27–30.
- Rothfels K, Milacic M, Matthews L, Haw R, Sevilla C, Gillespie M, et al. Using the reactome database. *Curr Protoc* 2023;3:e722.
- Sollis E, Mosaku A, Abid A, Buniello A, Cerezo M, Gil L, et al. The NHGRI-EBI GWAS Catalog: knowledgebase and deposition resource. *Nucleic Acids Res* 2023;51:D977–85.
- Wang QF, Su GN, Tan X, Deng J, Du L, Huang XY, et al. UVEOGENE: an SNP database for investigations on genetic factors associated with uveitis and their relationship with other systemic autoimmune diseases. *Hum Mutat* 2019;40:258–66.
- Stelzer G, Rosen N, Plaschke I, Zimmerman S, Twik M, Fishilevich S, et al. The GeneCards suite: from gene data mining to disease genome sequence analyses. *Curr Protoc Bioinformatics* 2016;54: 1–3.
- Dendrou CA, Petersen J, Ross J, Fugger L. HLA variation and disease. *Nat Rev Immunol* 2018;18:325–39.
- Goverdhan SV, Howell MW, Mullins EF, Osmond C, Hodgkins PR, Self J, et al. Association of HLA class I and class II polymorphisms with age-related macular degeneration. *Invest Ophthalmol Vis Sci* 2005;46:1726–34.
- Wakefield D, Clarke D, McCluskey P. Recent developments in HLA B27 anterior uveitis. *Front Immunol* 2020;11:608134.
- Kuiper JJW, Venema WJ. HLA-A29 and birdshot uveitis: further down the rabbit hole. *Front Immunol* 2020;11:599558.
- Song H, Liu BY, Huai WW, Yu ZX, Wang WW, Zhao J, et al. The E3 ubiquitin ligase TRIM31 attenuates NLRP3 inflammasome activation by promoting proteasomal degradation of NLRP3. *Nat Commun* 2016;7:13727.
- Guo YF, Lin P, Hua YM, Wang C. TRIM31: a molecule with a dual role in cancer. *Front Oncol* 2022;12:1047177.
- Zariwala MA, Knowles MR, Leigh MW. Primary ciliary dyskinesia. In: Adam MP, Feldman J, Mirzaa GM, Pagon RA, Wallace SE, Amemiya A, editors. *GeneReviews*® Seattle: University of Washington; 1993.
- Zhu DL, Zhang HG, Wang RX, Liu XJ, Jiang YT, Feng T, et al. Association of DNAH11 gene polymorphisms with asthenozoospermia in Northeast Chinese patients. *Biosci Rep* 2019;39:BSR20181450.

31. Xia H, Huang XJ, Deng S, Xu HB, Yang Y, Liu X, et al. DNAH11 compound heterozygous variants cause heterotaxy and congenital heart disease. *PLoS One* 2021;16:e0252786.
32. Verma S, Bakshi D, Sharma V, Sharma I, Shah R, Bhat A, et al. Genetic variants of DNAH11 and LRFN2 genes and their association with ovarian and breast cancer. *Int J Gynaecol Obstet* 2020;148:118–22.
33. Wang JR, Wang QZ, Wei B, Zhou Y, Qian ZY, Gao Y, et al. Intronic polymorphisms in genes LRFN2 (rs2494938) and DNAH11 (rs2285947) are prognostic indicators of esophageal squamous cell carcinoma. *BMC Med Genet* 2019;20:72.
34. Tam V, Patel N, Turcotte M, Bossé Y, Paré G, Meyre D. Benefits and limitations of genome-wide association studies. *Nat Rev Genet* 2019;20:467–84.